Correction of Mutant p63 in EEC Syndrome Using siRNA Mediated Allele-Specific Silencing Restores Defective Stem Cell Function

Vanessa Barbaro, Annamaria A. Nasti, Claudia Del Vecchio, Stefano Ferrari, Angelo Migliorati, Paolo Raffa, Vincenzo Lariccia, Patrizia Nespeca, Mariangela Biasolo, Colin E. Willoughby, Diego Ponzin, Giorgio Palù, Cristina Parolin, Enzo Di Iorio

STEM CELLS®

REGENERATIVE MEDICINE

Correction of Mutant p63 in EEC Syndrome Using siRNA Mediated Allele-Specific Silencing Restores Defective Stem Cell Function

VANESSA BARBARO,[a] ANNAMARIA A. NASTI,[b] CLAUDIA DEL VECCHIO,[b] STEFANO FERRARI,[a] ANGELO MIGLIORATI,[b] PAOLO RAFFA,[b] VINCENZO LARICCIA,[c] PATRIZIA NESPECA,[b] MARIANGELA BIASOLO,[b] COLIN E. WILLOUGHBY,[d] DIEGO PONZIN,[a] GIORGIO PALÙ,[b] CRISTINA PAROLIN,[b] ENZO DI IORIO[a,b]

Key Words. p63 • Ectrodactyly-ectodermal dysplasia-clefting syndrome • Epithelial stem cells • small interfering RNAs • Gene therapy

[a]Research Centre, Fondazione Banca degli Occhi del Veneto, 30174 Venice, Italy; [b]Department of Molecular Medicine, University of Padua, 35121 Padua, Italy; [c]Department of Biomedical Sciences and Public Health, School of Medicine, University "Politecnica delle Marche", 60120 Ancona, Italy; [d]Department of Eye and Vision Science, Institute of Ageing and Chronic Disease, University of Liverpool, Liverpool, United Kingdom

Correspondence: Enzo Di Iorio, Ph.D., Department of Molecular Medicine, University of Padua, 35121 Padua, Italy. Telephone: + 39-0498272345; + 39-3402357372; e-mail: enzo.diiorio@fbov.it

Received July 27, 2015; accepted for publication January 1, 2016; first published online in STEM CELLS *EXPRESS* February 17, 2016.

1066-5099/2016/$30.00/0

http://dx.doi.org/10.1002/stem.2343

ABSTRACT

Ectrodactyly-Ectodermal dysplasia-Clefting (EEC) syndrome is a rare autosomal dominant disease caused by heterozygous mutations in the *p63* gene and characterized by limb defects, orofacial clefting, ectodermal dysplasia, and ocular defects. Patients develop progressive total bilateral limbal stem cell deficiency, which eventually results in corneal blindness. Medical and surgical treatments are ineffective and of limited benefit. Oral mucosa epithelial stem cells (OMESCs) represent an alternative source of stem cells capable of regenerating the corneal epithelium and, combined with gene therapy, could provide an attractive therapeutic avenue. OMESCs from EEC patients carrying the most severe p63 mutations (p.R279H and p.R304Q) were characterized and the genetic defect of p.R279H silenced using allele-specific (AS) small interfering RNAs (siRNAs). Systematic screening of locked nucleic acid (LNA)-siRNAs against R279H-p63 allele in (i) stable WT-ΔNp63α-RFP and R279H-ΔNp63α-EGFP cell lines, (ii) transient doubly transfected cell lines, and (iii) p.R279H OMESCs, identified a number of potent siRNA inhibitors for the mutant allele, which had no effect on wild-type p63. In addition, siRNA treatment led to longer acquired life span of mutated stem cells compared to controls, less accelerated stem cell differentiation in vitro, reduced proliferation properties, and effective ability in correcting the epithelial hypoplasia, thus giving rise to full thickness stratified and differentiated epithelia. This study demonstrates the phenotypic correction of mutant stem cells (OMESCs) in EEC syndrome by means of siRNA mediated AS silencing with restoration of function. The application of siRNA, alone or in combination with cell-based therapies, offers a therapeutic strategy for corneal blindness in EEC syndrome. STEM CELLS *2016;34:1588–1600*

SIGNIFICANCE STATEMENT

The Ectrodactyly-Ectodermal dysplasia-Clefting (EEC) syndrome is a rare genetic disorder resulting from mutations in the *p63* gene and characterized by ocular surface defects. Cell therapy treatments based on transplantation of autologous corneal stem cells are not feasible for EEC patients as both eyes are affected and corneal limbus severely compromised. Epithelial stem cells deriving from the oral mucosa can be harvested with no limitations and grafts of oral mucosa are normally used in ophthalmology to repair the ocular surface. However, being the EEC syndrome a genetic disorder, cells will have to be genetically modified. Our genetic strategy could provide a therapeutic window to correct the EEC defect and counteract the clinical downstream effects of limbal stem cell deficiency.

INTRODUCTION

Ectrodactyly-Ectodermal dysplasia-Clefting (EEC) syndrome (MIM#604292) is an autosomal-dominant ectodermal dysplasia resulting from mutations in the *p63* gene and characterized by limb defects, orofacial clefting, ectodermal dysplasia, and ocular defects. *p63* is a transcription factor essential for the regenerative proliferation of epithelial stem cells in the skin and cornea. A healthy corneal epithelium is vital to maintain the transparency and refractive state of the cornea, which are essential for normal vision and ocular comfort. The corneal epithelium is a stratified epithelium from which superficial terminal cells are naturally shed, and the

lost corneal epithelial cells are replaced by stem cells located at the edges of the cornea, in a region known as the limbus. The stem cells for the corneal epithelium are, therefore, more commonly known as limbal epithelial stem cells (LESCs) because of their anatomical location. The *p63* gene generates six isoforms and ΔN*p63α* is the predominant isoform in the human corneal epithelium [1]. ΔN*p63α* is necessary for the maintenance of the proliferative potential of LESCs and essential for regenerative proliferation in the ocular surface. The major cause of visual morbidity in EEC syndrome is limbal stem cell deficiency (LSCD) and we recently reported that the diminished ability of LESCs to regenerate fully stratified corneal epithelia is related to *p63* mutations [2, 3].

LSCD is characterized by conjunctival epithelial ingrowth, neovascularization, recurrent corneal erosion, and persistent ulcers, as well as corneal scarring [2, 4] and ultimately leads to visual impairment and blindness. Transplantation of autologous LESC grafts has shown to be successful for the treatment of acquired unilateral LSCD, but it is not feasible in cases of bilateral LSCD, as in the EEC syndrome [5, 6]. Transplantation of allogenic limbal epithelium is possible, but requires systemic immunosuppression and it has a success rate that decreases gradually over time (graft survival rate of 40% at 1 year and 33% at 2 years) [7]. For patients with bilateral LSCD, transplantation of cultured autologous oral mucosal epithelial cell sheets might be the only effective alternative for reconstructing the ocular surface [8, 9]. Numerous studies have shown that oral mucosal epithelial stem cells (OMESCs) are a feasible alternative to limbal transplants [8–10], and an ideal substitute of LESCs in ocular surface reconstruction [11].

Given that five *p63* mutations account for almost 90% of EEC cases and that the arginine (R) residues at position 304 (R304) and 279 (R279) are mutational hotspots, gene silencing or editing strategies are required for a limited number of targets, making this approach an efficient strategy applicable to the majority of EEC patients. As EEC syndrome results from heterozygous dominant-negative mutations in the *p63* gene therapeutic strategies based on allele-specific (AS) gene silencing through RNAi could specifically inhibit the expression of disease-associated alleles without suppressing the expression of the corresponding wild-type (WT) alleles to phenotypically correct the stem cell population restoring function. Here, we characterize OMESCs from patients with EEC syndrome and demonstrate a proof-of-principle approach to correct the underlying genetic defect by AS gene silencing. Phenotypic correction of mutant *p63* in OMESCs using small interfering RNA (siRNA) mediated AS silencing restored full thickness stratification and differentiation of the epithelia. This study supports the application of siRNA, alone or in combination with cell based therapies as a therapeutic strategy for corneal blindness in EEC syndrome.

Materials and Methods

Cell Culture

Primary human keratinocytes were isolated from fresh oral mucosal biopsies of a healthy subject (aged 24) and two EEC patients (both patients were 18 years old) after an informed consent form was signed. The research program and the informed consent forms were approved by the Venetian Ethical Committee for Clinical Research Studies (Prot. 2009/77661, November 19, 2009). Once isolated, cells were cultivated as previously described [12, 13]. The calculation method used for cell doublings and cumulative population doublings was: $3{,}322*\log_{10}$ (UCY/I), where UCY = the cell yield at that point and I = number of clonogenic cells. The clonogenic cells were calculated as the cell number used as inoculum to begin that subculture multiplied by the colony forming efficiency (CFE) value. Human embryonic kidney cells stably transduced to express the simian virus 40 T antigen (293T) were provided by D. Baltimore (Rockefeller University, New York, NY).

Cell Proliferation Assay

The assay was performed in Silicone Culture-Insert in a 35-mm dish that creates a 0.5-mm gap across the diameter of the well (Ibidi, Madison, WI). Primary cells were cultured until confluence, then the insert was removed and the cell proliferation across the gap monitored over time using A1Rsi + Laser Scanning Confocal Microscopy (Nikon Instruments Inc., Melville, NY).

$[Ca^{2+}]_i$ Measurements

$[Ca^{2+}]_i$ was measured by single-cell computer-assisted videoimaging using A1Rsi + Laser Scanning Confocal Microscopy (Nikon Instruments Inc., Melville, NY), as described before [14]. Briefly, 3.5×10^5 OMESCs cells were plated one day prior to transfection on glass coverslips, covered with UV-irradiated 3T3 cells, in 35-mm dishes. Cells were loaded with 4 μM Fluo-4/AM (Molecular Probes, San Diego, CA; stock solutions of 1 mM in dimethyl sulfoxide (DMSO), stored in aliquots at −20 °C). Transfected cells were visualized using a 543-nm laser line (emission 570–600 nm) and selected for analysis. Images were acquired every 4 s and stored for offline analysis. Twenty to thirty-five individual cells were selected and monitored simultaneously from each coverslip. Fluo-4 fluorescence intensity was expressed as an F_i/F_{basal}-ratio, where F_i is the background subtracted fluorescence intensity and F_{basal} is the background subtracted mean fluorescence value measured from each cell at rest. All experiments were performed at room temperature.

Hemicornea Preparation In Vitro

Human Keratoplasty Lenticules (HKLs) were prepared as previously described [15]. Briefly, corneoscleral rims were preserved at 4 °C and used within 1–2 days from their excision. Each specimen was firmly placed in an artificial chamber and the epithelium manually removed after bathing the surface of the cornea with an isotonic solution containing 5 mg/ml of trypsin and 2 mg/ml of EDTA HKLs were obtained by microkeratome resection of epithelium-free corneas. Epithelial stem cells were plated onto HKLs at a concentration of 5×10^4 cells/cm^2. Hemicorneas were cultured under submerged conditions for 7 days and air-lifted for 14 further days.

Histology and Immunofluorescence

Hemicorneas were fixed in 4% paraformaldehyde, embedded in Optimal Cutting Temperature compound, frozen, and sectioned. Sections (5–7 μm) were analyzed using antibodies against ΔNp63α (rabbit polyclonal, 1:200; PRIMM, Milan, Italy), keratin 3 (AE5 clone, mouse monoclonal, 1:100; MP Biomedicals, Solon, OH), 14-3-3σ (rabbit polyclonal, 1:400; PRIMM), involucrin (goat polyclonal, 1:100; Santa Cruz Biotechnology, Santa Cruz, CA), laminin-β3 (goat polyclonal, 1:200; Santa Cruz Biotechnology, Santa Cruz, CA)

and Ki67 (mouse monoclonal, 1:100, Dako, Glostrup, DK) for 1 h at 37 °C. Fluoroscein-isothiocyanate (FITC) and rhodamine-conjugated secondary antibodies (1:100; Santa Cruz Biotechnology, Santa Cruz, CA) were used. Nuclei were stained with far-red fluorescent DNA dye (DRAQ5, 1:1000, Cell Signaling Technology, Boston, MA). For fluorescence quantification experiments, monolayers of 6×10^4 cells were deposited on slides by means of Shandon CytoSpin 3 Cytocentrifuge. Specimens were analyzed with a Nikon CLSM.

Vectors

The human WT-ΔNp63α and R279H -ΔNp63α encoding regions were obtained by reverse transcriptase-polymerase chain reaction (RT-PCR) performed on total RNA from p.R279H-OMESCs, employing specifically designed primers containing BamHI (PB1) and PstI (R/C), respectively, at the 5′ and 3′ end and cloned into the pCR2.1 TOPO-TA cloning plasmid. The red fluorescent protein (RFP) encoding sequence was amplified from the pTAG-RFP-T plasmid [16], while the EGFP fragment was derived from pcDNA3.1eGFP by polymerase chain reaction (PCR). The obtained PCR fragments, containing the PstI and the EcoRV restriction sites at the 5′ and 3′ end, respectively, were cloned in the pCR2.1 TOPO-TA cloning plasmid leading to TOPO-RFP and TOPO-eGFP constructs, respectively. The internal ribosome entry site (IRES)-Blasticidine cassette was amplified by PCR using as a template the pWPI-blr employing primers IB5′, containing an EcoRV restriction site at the 5′ end and IB3′, containing an XhoI restriction site at the 3′ end [17]. The PCR fragment was cloned in the pcR2.1 TOPO-TA cloning plasmid (TOPO-IRES-BLAST). The final pCDNA 3.1-based plasmids were constructed by ligating into the backbone digested with BamH1-EcoRV, the WT-ΔNp63α or R279H-ΔNp63α BamHI-PstI fragments, derived from the pCR2.1-ΔNp63α or ΔNp63α R279H, respectively. Expression is driven by the CMV promoter. The lentiviral vectors were generated by digesting a pRRL.SIN-18.cPPT.CMV.GFP.WPRE backbone with BamHI-Sal I and the following fragments inserted: (i) WT-ΔNp63α or R279H-ΔNp63α as a BamHI-PstI fragment derived from the pCR2.1-ΔNp63α or ΔNp63α-R279H, respectively; (ii) RFP or EGFP cassette as a PstI-EcoRV fragment derived from TOPO-RFP or TOPO-EGFP, and (iii) EcoRV-XhoI fragment containing the IRES-Blasticidine obtained from the TOPO-IRES-Blasticidine. All the plasmid-cloned fragments were confirmed by sequencing.

Production of Lentiviral Particles

Production of third generation HIV-derived vectors was achieved by transient cotransfection of four plasmids into 293T epithelial cell line [18]. The HIV-derived packaging constructs were pMDLg/pRRE and RSV-Rev, which contain: (i) the group-specific antigen (gag) and *pol* genes under the control of a cytomegalovirus (CMV) promoter and polyadengylation site of the human β-globin gene; (ii) the *rev* cDNA. VSV G was expressed from pMD.G, meanwhile the transfer constructs expressing the human WT ΔNp63α-RFP or R279H-ΔNp63α-EGFP downstream CMV promoter were pRRL.SIN-18. Forty-eight hours after transient transfection of the four plasmids into HEK293T cells by Lipofectamine 2000 (Life Technologies, Carlsbad, CA), supernatants were collected and then stored at −80 °C.

Transduction with Recombinant HIV Particles

HEK293T cells were seeded onto 12-well tissue culture plates at a density of 4×10^5 and transduced with recombinant viral particles using a range of serial dilutions. After 3 days, DNAs were analyzed by quantitative PCR, calculating the copy number of HIV sequences using primers and probes for GAG and GADPH detection. Titers were around of 10^6–10^7 transducing units/ml for each viruses.

Development of Stable Human ΔNp63α Cell-Lines

HEK293T cells (6×10^6) were seeded onto 10-cm tissue culture plates and transduced with recombinant viral particles using a range of 0.5–1 multiplicity of infection (MOI). After 3 days, transduced cells were exposed to complete Dulbecco's modified Eagle's medium supplemented with Blasticidin S HCl, at a concentration of 10 μg/ml. After about 2 weeks of selection, the arising clones were detached and subcloned into 24-well plates for imaging selection. Clones showing a p63 nuclear staining comparable to that of primary keratinocytes were expanded for further characterization.

Western Blot

Whole cell lysates for western blot were analyzed with the following primary antibodies: pan-p63 (4A4, mouse monoclonal, 1:500, Dako, Milan, Italy), $p16^{ink4a}$ (mouse monoclonal antibody, 1:500, Exalpha Biologicals, Shirley, MA), ΔNp63α (rabbit polyclonal, 1:200; PRIMM, Milan, Italy), and GAPDH (rabbit polyclonal, 1:1000; Santa Cruz Biotechnology, Santa Cruz, CA). The band intensities were quantified using an Image J analysis software. The relative amount of p63 protein was normalized to glyceraldehyde 3-phosphate dehydrogenase (GAPDH).

Senescence β-Galactosidase Cell Staining

β-Galactosidase activity was carried out in H-OMESCs, p.R279H-OMESCs, and p.R304Q-OMESCs according to the manufacturer's instructions (Cell Signaling Technology, Danvers, MA).

Real-Time qPCR Assays

Total RNAs from primary keratinocytes and 293T cells were extracted and purified using the RNeasy Micro kit (Qiagen, Hilde, Germany). For the absolute ΔNp63α quantification (Ab-qPCR), the level of expression of the target gene was normalized to (GAPDH). For the relative gene expression analysis (Rel-qPCR), the difference in relative p63 expression was performed using the $2^{-\Delta\Delta Ct}$ method. GAPDH was used as internal control gene. The percentage of WT or mutated mRNA ΔNp63α expression was measured by means of allele-specific real time (AS-qPCR) assay [3]. Primers and probes are shown in Table 1.

siRNA Sequence Walk and Transfection

All possible siRNAs ($n = 19$) were designed to target the R279H-p63 mRNA region containing a single-nucleotide change (G-A at nucleotide position 953 resulting in the amino acid change, R279H). They: (i) have a sequence of 19 nucleotides; (ii) incorporate the locked nucleic acid (LNA); (iii) were obtained as single stranded from Exiqon (Exiqon, Vedbaek, Denmark) and prepared as reported [19]. All siRNAs were transfected into (i) 293T cells stably expressing either the human ΔNp63α or ΔNp63α-R279H, (ii) serially propagated primary keratinocytes, and (iii) organotypic cultures with Lipofectamine 2000 (Life Technologies, Carlsbad, CA).

Dose Titration Analysis

Titration of siRNA *a* was performed using a narrow range of siRNAs from 0.1 to 10 nM in 293T HEK ΔNp63α stable cell lines and from

Table 1. List of primers and probes used in Ab-qPCR and AS-qPCR

PB1	5′-CGCGGATCCGCTAACATGTTGTACCTGGAAAACAATGC-3′
R/C	5′-CCAATGCATTGGTTCTGCAGTCCCTCCCCCTCCTC-3′
5′RFP	5′-AAAACTGCAGGTGGTGTCTTAAGGGCGAAGAG-3′
3′RFP	5′-AAAACTGCAGGTGGTGTCTAAGGGCGAAGAG-3′
5′GFP/G	5′-AAAACTGCAGGTGGTGAGCAAGGGCGAG-3′
3′GFP	5′-GATATCTTACTTGTACAGCTCGTCC-3′
IB5′	5′-GATATCCGCCCCCCCCCCCTAACGTTAC-3′
IB3′	5′-CCGCTCGAGTTAGCCCTCCCACACATAACC-3′
GAG Fw	5′-GGAGCTAGAACGATTCGCAGTTA-3′
GAG Rev	5′-GGTTGTAGCTGTCCCAGTATTTGTC-3′
GAG Probe	5′-[6FAM]ACAGCCTCCTGATGTTTCTAACAGGCCAGG[BHQ1]-3′
GADPH Fw	5′-CCACTCCTCCACCTTTGACG-3′
GADPH Rev	5′-CATGAGGTCCACCACCCTGT-3′
GADPH Probe	5′-[TET]TTGCCCTCAACGACCACTTT[TAM]-3′
ΔNp63α Fw	5′-GCATTGTCAGTTTCTTAGCGAG-3′
ΔNp63αRev	5′-CCATGGAGTAATGCTCAATCTG-3′
ΔNp63α Probe	5′-[6FAM]GGACTATTTCACGACCCAGG[BHQ1]-3′
WT-ΔNp63α	5′-[6FAM]AATTGGACGGCGGTTCATCC[BHQ1]-3′
R279H-ANp63α	5′-[TET]AATTGGACGGTGGTTCATCCC[BHQ1]-3′

Abbreviations: Ab-qPCR, absolute quantitative PCR; ASqPCR, allele-specific quantitative PCR; GAG, group-specific antigen; GAPDH, glyceraldehyde 3-phosphate dehydrogenase; GFP, Green Fluorescence Protein; RFP, red fluorescent protein.

0 to 100 nM in OMESCs. Residual WT- and R279H-ΔNp63α protein levels was measured by means of laser scanning confocal microscopy, while transcript levels of WT and mutated R279H mRNAs were quantified by means of AS-qPCR. Concentration-response curves were obtained by fitting the data to the four parameter logistic equation $y = \min + (\max - \min)/(1 + (x/IC_{50})n)$, where y is the normalized value of real-time PCR or imaging values, x is the siRNA concentration in nanomoles per liter, and n is the Hill coefficient. Data fitting was obtained with the Origin software (OriginLab Ltd., Northampton, MA).

Statistical Analysis

All data are reported as mean ± S.E.M. When comparing two data sets, the Student's t test for unpaired data was used. To compare multiple groups, statistical comparisons were performed with one-way or two-ways ANOVA followed by Tukey-Kramer post hoc test. Significance is at $p < .05$. Statistical comparisons were carried out using the Graph-PAD 3.02 software suite (GraphPad Software Inc., San Diego, CA).

Results

p63-Defective Oral Epithelial Cells Undergo a Rapid Exhaustion of Clonogenic and Self-Renewal Potential, Resulting in Accelerated Ageing

To investigate how p.R279H and p.R304Q p63 mutations affect LESC physiology in EEC syndrome, OMESCs from healthy (H-OMESCs, $n = 1$) or EEC individuals (EEC-OMESCs, n = 2, with heterozygous p.R279H and p.R304Q p63 mutations) were isolated from oral mucosal biopsies and serially propagated until exhaustion. Compared to H-OMESCs, EEC-OMESCs showed (i) a more rapid decrease of CFE and clonogenic cell numbers (Fig. 1A, 1B), (ii) progressive increased percentage of aborted colonies during serial cultivation (Fig. 1C), and (iii) increased replicative senescence, as suggested by the lower number of cell passages in culture (Fig. 1D). As previously reported in papers describing the effects of the loss of p63 [20, 21], cell growth was faster in EEC-OMESCs, with cultures becoming confluent in 4–5 days compared to 6–7 days observed in H-OMESCs controls. In addition, we also observed that EEC-OMESCs proliferate at a faster rate compared to controls, both at 4 h or 7 h after the insert was removed (Fig. 1E). Percentage of wound closure was also increased in EEC-OMESCs compared with H-OMESCs; specifically H-OMESCs showed 1.0 ± 0.2% and 32 ± 4% closure at 4 h and 7 h, respectively, whereas p.R279H OMESCs showed 6 ± 1% and 58 ± 3% closure at 4 h and 7 h, respectively and p.R304Q OMESCs 15 ± 1% and 86 ± 7% closure at 4 h and 7 h, respectively (Fig. 1F). To demonstrate that p63 mutant cells undergo accelerated ageing, we performed a senescence-associated-beta galactosidase staining (Fig. 1G) and western blot of p16 and ΔNp63α at different cell passages (1 and 7) (Fig. 1H) in H-OMESCs, p.R279H-OMESCs, and p.R304Q-OMESCs.

Mutations in *p63* Lead to Abnormal Stratification of Epithelia and Differentiation Pathways

We evaluated the ability of p63-defective EEC-OMESCs to stratify and differentiate in a HKL model [15]. Primary healthy, p.R279H, and p.R304Q OMESCs at passage two were seeded onto HKLs and grown for 21 days. Compared to H-OMESCs controls, epithelia generated by EEC-OMESCs were hypoplastic with defects in epithelial thickness and cellularity with some areas devoid of cells and with flat irregular and terminally differentiated cells (Fig. 2A). Quantitatively, epithelial thickness was reduced when p.R279H OMESCs (mean: 12.1 ± 7 μm; maximum: 21.3 μm) or p.R304Q OMESCs (mean: 9.1 ± 3.0 μm; maximum: 14.5 μm) were compared to epithelia obtained from H-OMESCs (mean: 56.4 ± 18.0 μm; maximum: 82.3 μm). The number of cell layers in the epithelium was higher in HKLs seeded with H-OMESCs (mean: 3.9 ± 1.2 cell layers; maximum: 5.8 cell layers), compared to those with p.R279H OMESCs (mean: 1.2 ± 1.3 cell layers; maximum: 2.2 cell layers) and with p.R304Q OMESCs (mean: 1.1 ± 1.0 cell layers; maximum: 1.2 cell layers). Ultrastructural analyses with laser scanning confocal microscopy showed that epithelia from H-OMESCs were organized into (i) basal column-shaped cells expressing p63, (ii) flat squamous superficial terminally

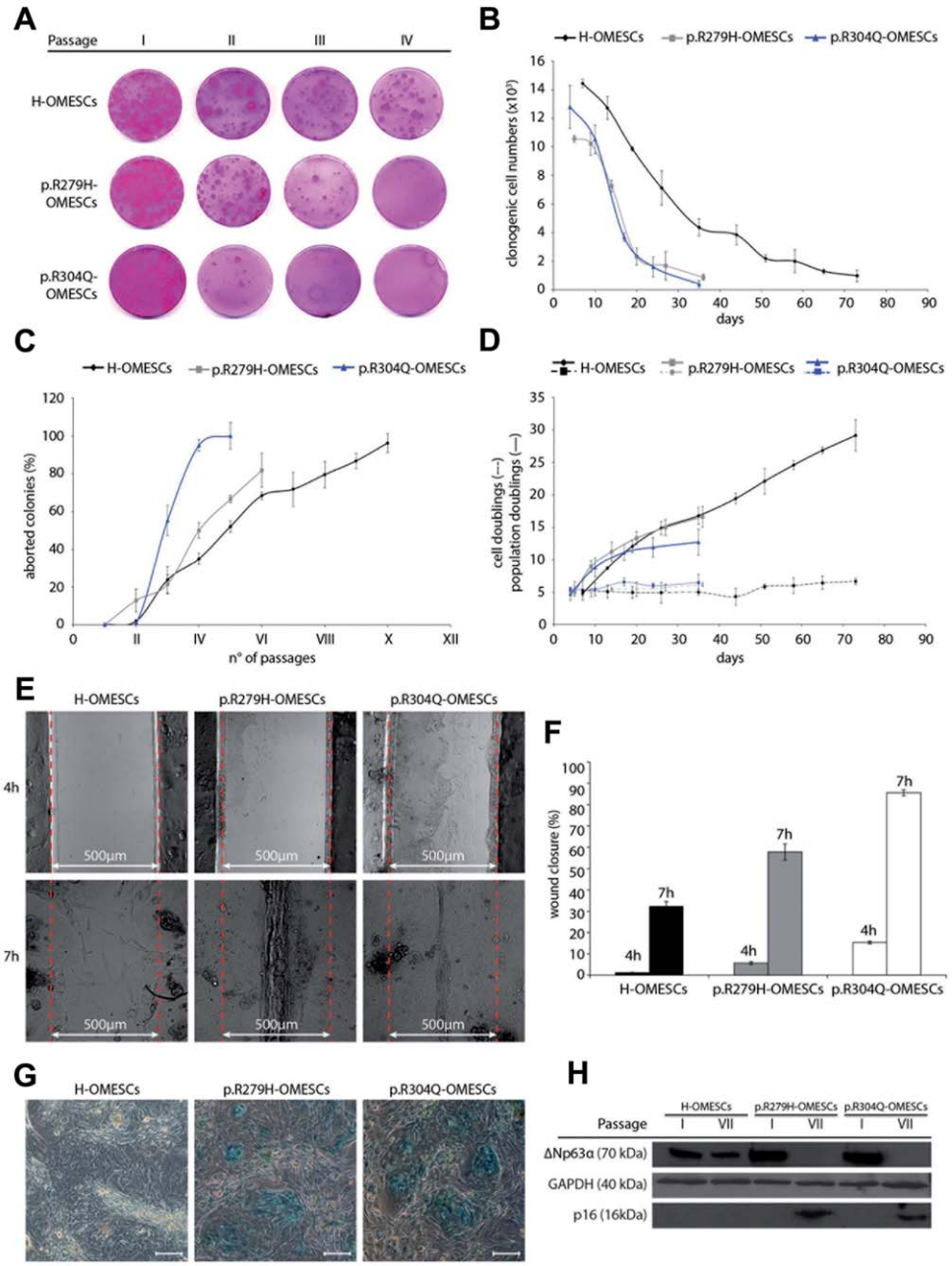

Figure 1. p.R279H and p.R304Q OMESCs show altered clonogenic ability and proliferative potential. Life-span analysis of OMESCs from healthy (H-) or p.R279H and p.R304Q ectrodactyly-ectodermal dysplasia-clefting (EEC) donors. Data have been obtained from three unrelated normal subjects and from biopsies of two unrelated EEC patients. **(A)**: Colony forming efficiency of healthy, p.R279H and p.R304Q OMESCs was evaluated at the cell passages indicated. Images are representative of data obtained from at least four independent experiments. Quantification of **(B)** clonogenic cells numbers, **(C)** percentage of aborted colonies, **(D)** cell doublings and cumulative population doublings of healthy (black line), p.R279H (gray line), and p.R304Q (blue line) OMESCs are shown. EEC-OMESCs were passaged 5–6 times (= 35–36 days) compared to the 11 passages, that is, 73 days in culture, seen in H-OMESCs controls. All data are expressed as mean ± SEM ($n = 3$ independent experiments). **(E)**: Cell proliferation assay of OMESCs from healthy or p.R279H and p.R304Q EEC donors. Images captured at 4 and 7 h after the silicon insert removing ($n = 3$ independent experiments). **(F)**: Quantification of the cell proliferation assay. Results are expressed as percentage of closure over the wound area ($n = 3$ independent experiments). **(G)**: Beta-galactosidase staining performed on H-OMESCs, p.R279H-OMESCs, and p.R304Q-OMESCs (scale bars = 200 μm). **(H)**: Western blot of ΔNp63α and p16 in H-OMESCs, p.R279H-OMESCs, and p.R304Q-OMESCs at different cell passages (1 and 7). Abbreviations: GAPDH, glyceraldehyde 3-phosphate dehydrogenase; OMESCs, oral mucosa epithelial stem cells; SEM, standard error of the mean.

differentiated cells, as indicated by the expression of keratin 3 and involucrin, (iii) suprabasal cuboid wing cells, expressing 14-3-3σ, an early differentiation marker for stratified epithelia, and (iv) proliferating cells, expressing Ki67 (Fig. 2B). The basal cuboidal cell layer was firmly attached to the underlying extracellular matrix and to the basement membrane (Fig. 2B, top panel). In contrast, tissues generated from EEC-OMESCs showed defects in both stratification and differentiation, thus resulting in severe tissue hypoplasia and lack of proper tissue polarity (Fig. 2B, middle and bottom panels), but not in

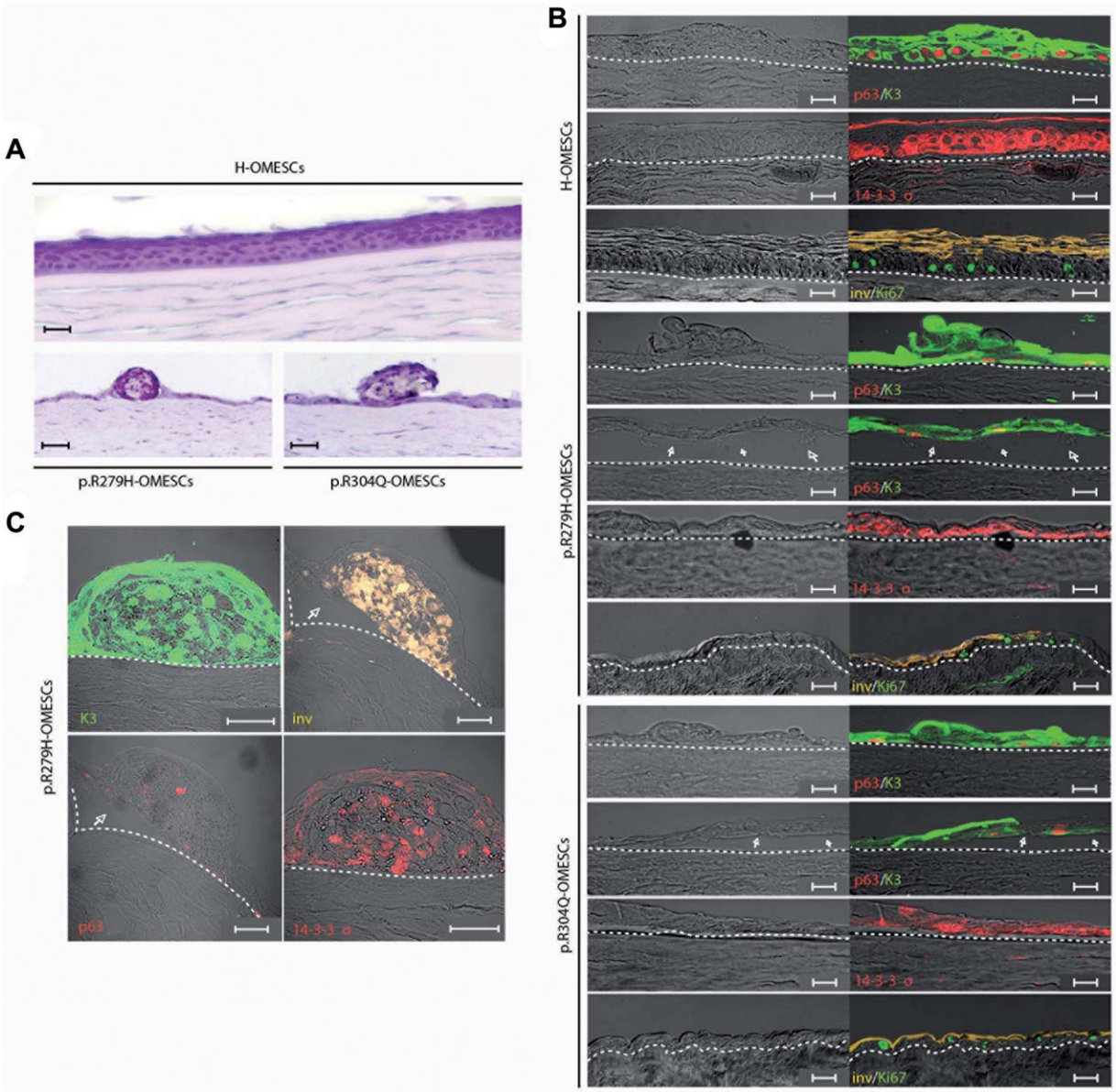

Figure 2. p.R279H and p.R304Q p63 mutations lead to abnormal epithelial stratification and differentiation pathways. **(A)**: Hematoxylin-eosin staining of epithelia generated on human keratoplasty lenticules by healthy, p.R279H and p.R304Q primary OMESCs at passage 2 ($n = 3$, scale bars = 50 μm). **(B)**: Double-immunofluorescence on epithelia derived from the above OMESCs using p63(red)/K3(green), 14-3-3σ (red, Ki67 (green), and involucrin (orange) antibodies ($n = 3$, scale bars = 20 μm). **(C)**: Immunofluorescence performed on the anomalous clusters of terminally differentiated p.R279H OMESCs using p63 (red), K3 (green), involucrin (orange), and 14-3-3σ (red) antibodies ($n = 3$, scale bars = 50 μm). Abbreviations: OMESCs, oral mucosa epithelial stem cells; K3, keratin 3.

proliferation (Ki67 is similar in EEC and healthy cells). We also observed anomalous clusters of terminally differentiated cells strongly expressing keratin 3 and involucrin (terminal differentiation marker for stratified epithelia), but not p63 and low 14-3-3σ, indicative of a premature terminal differentiation phenotype (Fig. 2C). As previously reported [22], we also observed reduced adhesion properties of the epithelium obtained by mutant cells (Fig. 2B, 2C).

Cells are known to progressively lose sensitivity to extracellular calcium as they proceed further along the differentiation process [23–30]. Since EEC-OMESCs display defective differentiation and stratification, we speculated that cellular calcium cycling is altered in cells expressing p63 mutants. Specifically, we analyzed capacitative calcium entry, one of the main calcium influx pathway of not-excitable cells, in H-OMESCs and EEC-OMESCs (at the third passage, when differentiation has already developed). When intracellular calcium store was depleted to activate capacitative channels [31], we found that, compared to H-OMESCs controls, the capacitative calcium entry was significantly reduced both in p.R279H and p.R304Q OMESCs, as a likely consequence of the premature accelerated differentiation of the mutated cells (Supporting Information Fig. 1).

ΔNp63α Expression in Cells from Healthy and p.R279H EEC Donors

Given that p63 accumulation, due to higher stability of the EEC mutated isoform, has been previously observed in tissues

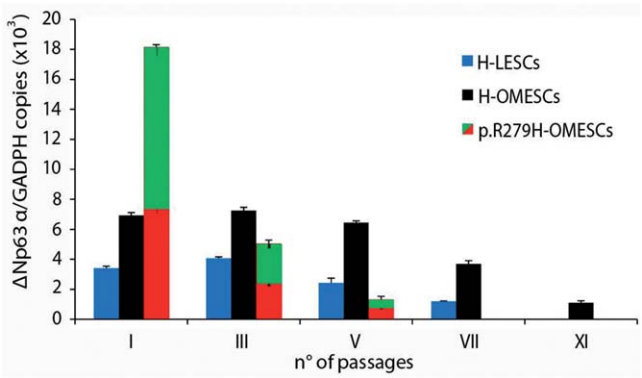

Figure 3. ΔNp63α expression in cells from healthy and p.R279H ectrodactyly-ectodermal dysplasia-clefting donors. Absolute quantitative PCR showing ΔNp63α copy number in total RNA from LESCs, H-, and p.R279H OMESCs, and allele-specific quantitative PCR (AS-qPCR) of R279H-p63 mutant during the passages. For the Ab-qPCR, results were normalized against GADPH. AS-qPCR data indicate the percentage of R279H-p63 allele compared to WT-p63. Data represent mean ± SEM. Abbreviations: GAPDH, glyceraldehyde 3-phosphate dehydrogenase; LESC, limbal epithelial stem cell; OMESCs, oral mucosa epithelial stem cells.

of patients affected by EEC syndrome [32], ΔNp63α expression in p.R279H OMESCs was quantified using an absolute quantitative PCR at different passages in culture (I, III, V, VII, and XI) and compared to H-OMESCs and healthy-limbal epithelial stem cells (H-LESCs). As shown in Figure 3, ΔNp63α decreased during serial cultivation, becoming very low after the seventh passage. The rate of reduction was faster in p.R279H OMESCs, compared to H-OMESCs and H-LESCs. ΔNp63α expression was threefold higher in p.R279H OMESCs compared to H-OMESCs, at the first passage. This correlates well with the abnormal hyperproliferation of p.R279H EEC primary cells, previously observed in the CFE and cell proliferation assays (Fig. 1A, 1E). This most likely results from an impaired negative regulatory loop, which is ΔNp63α-dependent, needed for cell-cycle arrest, and for the initiation of a differentiation program [33]. Importantly, the amount of ΔNp63α in primary H-LESCs was approximately two times lower than in H-OMESCs. This correlates well with their "cumulative population doubling ability" observed in vitro (H-LESCs = 10 ± 2 passages; H-OMESCs = 12 ± 2 passages) [34] and reflects the different "intrinsic lifespan" and "clonogenic potential" of the two cell lineages. Our findings confirm that ΔNp63α is a robust stem cell marker: (i) its expression declines during the differentiation and senescence processes of primary epithelia stem cells in vitro and (ii) also provide further evidences of the premature differentiation found in EEC-OMESCs. To gain greater insight into the relationship between ΔNp63α expression and EEC pathogenesis, we evaluated the percentage of WT or mutated mRNA p63 expression through allele-specific quantitative PCR (AS-qPCR). AS-qPCR demonstrated that the profile expression ratios of two transcripts were different in three passages analyzed (I, III, and V) with a decrease of the mutated p63 mRNA (Fig.3, green and red indicate mutant and WT expression levels, respectively). At the first passage, the percentages of mutant R279H p63 mRNA and WT p63 mRNA were 60 ± 7% and 40 ± 5% respectively, while during the differentiation process, these ratios decreased to 12 ± 1.7% and 23 ± 0.9%, respectively.

Establishment of a p.R279H EEC Model System

To screen the efficiency of siRNAs to block the expression of mutant p63 with little or no effect on WT p63, we established two cellular models stably expressing WT-ΔNp63α or R279H-ΔNp63α HEK293T cells, an epithelial cell line with no endogenous p63 expression, were transduced with third generation lentiviruses carrying WT- or R279H-ΔNp63α alleles fused to RFP or EGFP sequences, respectively (Fig. 4A). After the isolation of stable clones ($n = 14$ for both constructs), we observed that all the cell lines carrying the R279H-ΔNp63α allele showed higher levels of ΔNp63α expression, at the mRNA expression level, than control clones expressing WT-ΔNp63α (Supporting Information Fig. 2A). Considering that (i) both WT than R279H-ΔNp63α cell lines were obtained using the same transduction and selection conditions and (ii) the same results were also obtained after transient transfection, the hypothesis is that our cell model mirrors the higher amount of R279H-ΔNp63α, previously found and described ex vivo in p.R279H OMESCs. To test our hypothesis and screen the ability of siRNAs to counteract the R279H-p63 expression, we chose two clones (WT#9 and R279H#2) that exhibited the typical nuclear localization signal of ΔNp63α and expressed, *in toto*, mRNA and protein levels of ΔNp63α comparable to the endogenous level found in EEC-OMESCs (Supporting Information Fig. 2A, 2B).

Systematic Screening of LNA-siRNAs Against the R279H-*p63* Allele

Stable cell lines were used to separately transfect a collection of 19 LNA siRNAs [35, 36], designed to target the R279H-p63 mRNA region containing the single nucleotide change. Forty-eight hours post siRNA transfection, AS downregulation was assessed through ΔNp63α relative-qPCR. siRNAs (*a, b*, and *c*) specifically downregulated the R279H-ΔNp63α mRNA by approximately 90% (Fig. 4B). Interestingly, some siRNAs upregulated R279H-ΔNp63α (*r* and *s*), suggesting an interference with the ΔNp63α post-transcriptional regulation pathway. No changes in cell viability were observed after siRNA transfection. Western-blot analyses demonstrated a significant and specific reduction of mutant ΔNp63α protein when siRNA *a* was used (45 ± 4%), while protein downregulation with siRNA *b* and siRNA *c* did not have consistent and reproducible effects (Fig. 4C, 4D). Imaging analyses of the two HEK293T-ΔNp63α stable lines treated with doses of siRNA *a* ranging from 0 to 10 nM (0, 0.1, 1, and 10 nM) showed that compared to a nontargeting control siRNA (siNCT; negative control), siRNA *a* (i) reduced the expression of R279H-ΔNp63α-EGFP protein in a concentration-dependent way, reaching 43 ± 5% at 10 nM, (ii) maintained the fluorescence of the WT-ΔNp63α-RFP protein, and (iii) had an IC_{50} of 3.15 ± 0.79 nM, showing a potent inhibitory effect in vitro (Supporting Information Fig. 2C-2E).

To evaluate the specificity of siRNA *a* to (1) inhibit the R279H-ΔNp63α neo-synthesis, and (2) downregulate its expression in time-dependent manner, we utilized transiently transfected HEK293T cell lines, as an in vitro cellular model of the EEC disease-related heterozygous state. The HEK293T cell line was cotransfected with a 1:1 ratio of both WT-ΔNp63α-RFP and mutant ΔNp63α-EGFP plasmids in the presence of the siRNA *a*. We observed a specific and significant neo-synthesis inhibition of R279H-ΔNp63α-EGFP expression in approximately 80% of total cells at 48 h post transfection when compared to siNCT-

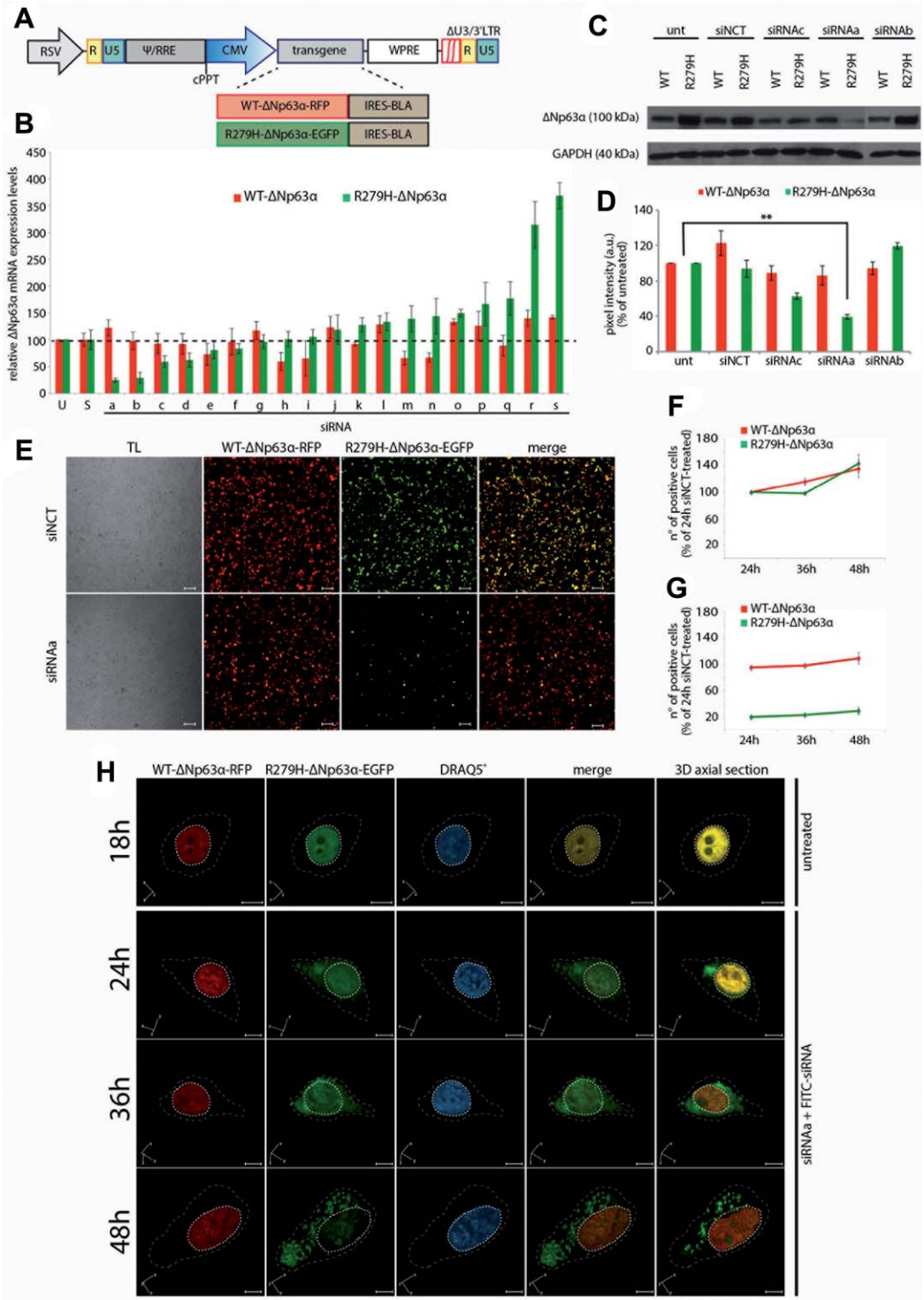

Figure 4. siRNA *a* specifically inhibits R279H-ΔNp63α expression in a time-dependent manner in ΔNp63α expressing cell lines. **(A)**: Third generation HIV-derived vectors include a modified 5′ and 3′ LTR, a packaging signal (ψ), RRE, and central polypurine tract (PPT). WT- or R279H ΔNp63α-cDNAs have stop codons fused to RFP or Green Fluorescence Protein (GFP), respectively, followed by IRES and blasticidin resistant gene. **(B)**: Relative-qPCR showing ΔNp63α mRNA downregulation in RNAs extracted from WT-ΔNp63α and R279H-ΔNp63α HEK293T stable cell lines either untreated (U) or transfected with control (S) or ΔNp63α siRNAs at 10 nM. **(C)**: Immunoblot detection of ΔNp63α in WT- and R279H-ΔNp63α HEK293T cells transfected with control (siNCT) or selected ΔNp63α siRNAs ($n = 5$). **(D)**: Western blot quantification shows ΔNp63α levels in the WT-ΔNp63α and R279H-ΔNp63α HEK293T cells. Data are expressed as mean ± SEM ($n = 5$). $^{**}p < .01$. **(E)**: Scanning confocal microscope analyses of HEK293 cells transiently transfected with WT-ΔNp63α-RFP and R279H-ΔNp63α-EGFP plasmids, in combination with siNCT or siRNAa, 48 h post-transfection. TL indicates transmitted light, red indicates RFP-fused WT-ΔNp63α protein, green indicates EGFP-fused R279H-ΔNp63α isoform and yellow indicates colocalization of both isoforms (magnification = ×10; scale bars = 100 μm). **(F)**: Time-point fluorescence quantification of WT-ΔNp63α-RFP and R279H-ΔNp63α-EGFP transiently expressed in HEK293T cells, cotransfected with siNCT. Data are expressed as mean ± SEM ($n = 4$ independent experiments). **(G)**: Time-point quantification of protein fluorescence of WT-ΔNp63α-RFP and R279H-ΔNp63α-EGFP transiently expressed in HEK293T cells, cotransfected with siRNA *a*. Data are expressed as mean ± SEM ($n = 4$ independent experiments). **(H)**: Z-stack (3D) and orthogonal fluorescent images of HEK293T cells transiently transfected with WT-ΔNp63α-RFP and R279H-ΔNp63α-EGFP plasmids, and treated with a combination of fluorescein isothiocyanate (FITC)-siRNA and siRNA *a*, 18 h post-transfection (time-points indicate hours from the WT-ΔNp63α-RFP and R279H-ΔNp63α-EGFP plasmids transfection; magnification = ×300; scale bars = 10 μm). Red indicates RFP-fused WT-ΔNp63α protein, green indicates EGFP-fused R279H-ΔNp63α isoform and FITC-siRNA and blue indicates nuclei of cells stained with DRAQ5. Abbreviations: EGFP, enhanced green fluorescent protein; GAPDH, glyceraldehyde 3-phosphate dehydrogenase; LTR, long terminal repeat; RFP, red fluorescent protein; RRE, *rev* response element; siRNA, small interfering RNA; WT, Wild type.

treated cells (Fig. 4E-4G). In further experiments, siRNA *a* was subsequently added to transiently cotransfected cells, together with fluorescein labeled siRNA (FITC-siRNA) to follow the delivery of the siRNAs. Z-stack imaging and orthogonal analyses of the fluorescent cells showed a specific time-dependent silencing of R279H-ΔNp63α-EGFP. Forty-eight hours post transfection a maximum effect was observed in siRNA *a* + FITC-siRNA targeted cells (Fig. 4H). We further wanted to validate the inhibitory potential of our most discriminating and potent AS siRNAs ex vivo. To estimate the transfection efficiency of siRNAs in human OMESCs and to allow direct observation of their cellular uptake, distribution, and localization, primary p.R279H OMESCs were transfected using concentrations of FITC-siRNA ranging from 10 to 100 nM (10, 25, 50, 75, and 100 nM). Forty-eight hours post transfection, the optimal transfection efficiency was of 88 ± 2% at 100 nM (Fig. 5A). Subsequently, we serially transfected the siRNA *c*, siRNA *a*, and siRNA *b* in the primary p.R279H OMESCs at 100 nM, and the expression levels of WT and R279H-p63

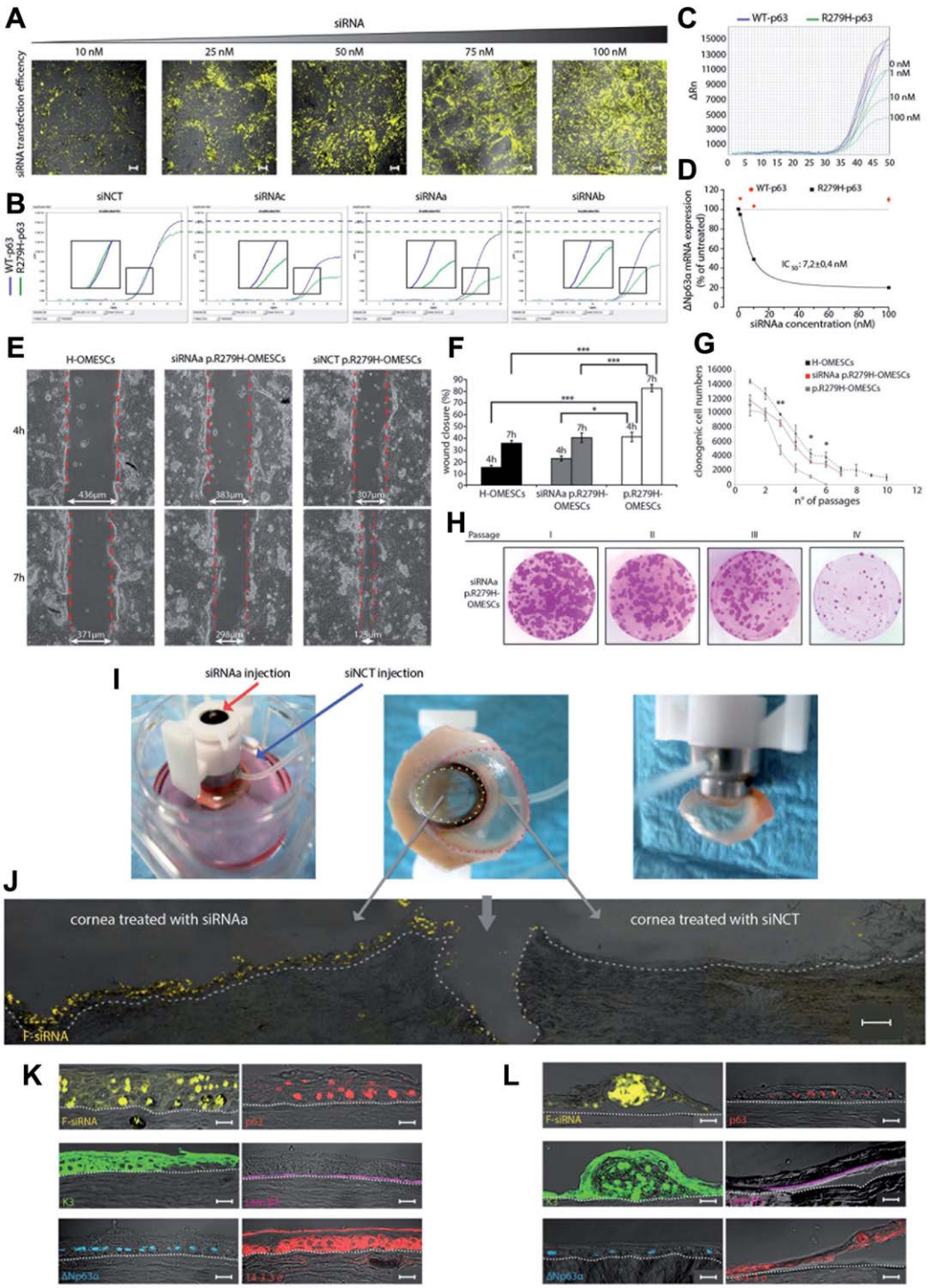

were measured using AS-qPCR. Amplification plots of WT (blue curves) and mutated mRNA (green curves) output from (i) siNCT, (ii) siRNA *c*, (iii) siRNA *b*, (iv) siRNA *a*, and (v) the H-OMESCs samples are shown in Figure 5B. Significant suppression of mutant mRNA occurred with siRNA *a*, and also with siRNA *b* and *c*, which suppressed mutant mRNA levels up to 80%, 72%, and 65% with respect to untreated cells, respectively. To determine the minimum concentration of siRNA *a* needed to knockdown the R279H-p63 mRNA, a dose-response (concentration) analysis was performed within a narrow range of 0, 1, 10, and 100 nM and the transcript levels evaluated with AS-qPCR. As shown in Figure 5C, titration of siRNA *a* abolished the R279H mRNA, showing a gradient of values which correlated with the concentration used, with an IC_{50} of 7.20 ± 0.04 nM (Fig. 5D). siRNA *a* was, therefore, able to downregulate the mutated allele without altering the expression of the WT-ΔNp63α both in vitro and ex vivo.

Restoration of Premature Clonogenic and Proliferative Arrest in R279H-p63 Primary Cells by Long-Term siRNA *a* Treatment

To investigate whether siRNA *a* could restore the functional phenotype in p.R279H OMESCs, we repeated the cell proliferation assays with OMESCs treated with either siNCT or siRNA *a* (at 100 nM). Imaging analyses revealed that the wound closure at 4 and 7 h was reduced in p.R279H OMESCs treated with siRNA *a*, but not with siNCT, and the closure kinetics were more similar to control H-OMESCs (Fig. 5E, 5F). Furthermore, p.R279H OMESCs treated with siRNA *a* (but not with siNCT) had a longer life-span and were able to be passaged in culture seven times compared to 5–6 with H-OMESCs. Finally, siRNA *a* treatment specifically mitigated the progressive loss of clonogenic cells in p.R279H OMESCs, and a trend more similar to H-OMESCs was achieved (Fig. 5G), as also confirmed by the results of the CFE assay (Fig. 5H). At the concentration of siRNA used, no significant alterations were observed in both the keratinocyte morphology and the expression level of markers such as p63, ΔNp63α, MUC1, K3, K4, and K13 in siRNA *a*-treated OMESCs.

Impaired Epithelial p.R279H OMESCs Stratification and Differentiation is Rescued by siRNA *a* Infusion

To test the ability of siRNA *a* to restore the epithelial tissue phenotype, two simultaneous organotypic cultures of p.R279H OMESCs were established using a device able to create two different and separated areas in a single HKL (Fig. 5I). One area was treated with siRNA *a* and the adjacent with a scrambled siRNA (siNCT) (Fig. 5J). FITC-siRNAs were also added to track distribution. At the end of the culture, histological sections of the tissues were taken to assess the ability of p.R279H OMESCs to correctly stratify following siRNA *a* treatment (Fig. 5K) and compared to control (Fig. 5L). Confocal microscopy demonstrated the presence of a well-organized and stratified epithelium of 4–5 layers limited to the area treated with siRNA *a*, while the adjacent region showed the typical phenotype of the p63-mutated cells. The resulting epithelium was characterized by basal expression of p63 and ΔNp63α while expression of keratin 3 and 14-3-3σ was mainly found in the upper cell layers. The basal cuboidal epithelial cells were anchored to the basement membrane and expressed β3-laminin.

Discussion

AS gene silencing has previously been described for the treatment of Amyotrophic Lateral Sclerosis [37, 38] and other genetic diseases [39, 40]. For the cornea, AS siRNAs have been successfully developed against the mutant allele of the KRT12 gene for a severe form of Meesmann Epithelial Corneal Dystrophy [41]. AS siRNAs represent a potential approach to treat the heterozygous dominant-negative *p63* mutations which result in EEC syndrome and corneal blindness due to LSCD.

In this study, we characterized OMESCs from patients with EEC syndrome and demonstrated a proof-of-principle approach

Figure 5. siRNA *a* restores the epithelial phenotype, stratification and differentiation properties of p.R279H OMESCs. **(A)**: Scanning confocal microscope images of p.R279H OMESCs transfected using fluoroscein-isothiocyanate (FITC)-siRNAs ranging from 10 to 100 nM (10, 25, 50, 75, and 100 nM). Forty-eight hours post-transfection, the optimal transfection efficiency was of $88 \pm 2\%$ at 100 nM. Yellow indicates FITC-fused scramble siRNA (magnification: × 10; scale bars: 50 μm). **(B)**: Four representative allele-specific quantitative PCR (AS-qPCR) plots of WT- and R279H-p63 mRNA expression in p.R279H OMESCs transfected with 100 nM of siNCT or siRNA *c*, siRNA *a*, or siRNA *b*. Both Ct and end-point values of the R279H-ΔNp63α mRNA are correlated with the mutated allele silencing, reaching respectively the 72%, 80%, and 65%. Violet indicates WT- and green indicates R279H-p63 mRNAs. **(C)**: A representative AS-qPCR plot of WT-p63 and R279H-p63 expression in p.R279H OMESCs transfected with a range of 0, 1, 10, and 100 nM of siRNA *a*, 48 h post-transfection. Image is representative of data obtained from at least three independent experiments. Violet indicates WT-p63 mRNA and green indicates R279H mRNA. **(D)**: Concentration-response curves of WT- and R279H-ΔNp63α mRNAs values in OMESCs, obtained from at least three independent AS-qPCR experiments. The value of the Hill coefficient was 1.54 ± 0.7. **(E)**: Laser scanning confocal microscope images of the wound healing assay, performed on healthy (H-OMESCs) and ectrodactyly-ectodermal dysplasia-clefting donors cells (p.R279H-OMESCs), with control (siNCT) or siRNA *a* treatment, at the indicated time after the silicone insert was removed. Images are representative of at least two independent experiments. **(F)**: Quantification of the wound closure assay. Data indicate the percentage of the wound closure relative to the total area of the scratch. All data are expressed as mean ± SEM and derived from at least two independent experiments. $*p < .05$, $***p < .001$. **(G)**: Colony forming efficiency (CFE) assay of WT-p63 and p.R279H OMESCs, continuously exposed to siNCT or siRNA *a*, evaluated at the cell passages indicated. siRNA *a* effectively reestablishes the clonogenic ability and proliferation property of the p63 mutant cells. All data are expressed as mean ± SEM and derived from at least three independent experiments. $*p < .05$, $**p < .01$. **(H)**: CFE assay at passages I to IV after treatment of p.R279H OMESCs cells with siRNA a. **(I)**: Photos of the device used to create two different areas in human keratoplasty lenticules. Red line indicates the area treated with siRNA *a*, the yellow line indicates the area treated with a control siRNA (siNCT), both in combination with a yellow fluorescent placebo siRNA (F-siRNA). **(J)**: Hystological images of organotypic cultures made with p.R279H OMESCs, treated for at least 2 weeks with siRNA *a* or siNCT, in combination with the fluorescent siRNA. The continuous infusion of siRNA *a* induces the proper stratification and differentiation of p.R279H cells. Images of cells containing the yellow fluorescent molecule indicate that cells actively divided after siRNA *a* treatment; scale bars: 100 μm. Magnification of immunofluorescence images from organotypic cultures treated with siRNA *a* **(K)** or with a scrambled siRNA **(L)** obtained with pan-p63, ΔNp63α; β3-laminin, and 14-3-3σ show the appropriate expression of these proteins. Images are representative of data obtained from at least three independent experiments. Scale bars = 20 μm. Abbreviations: F-siRNA, FITC-small interfering RNA; OMESCs, oral mucosa epithelial stem cells; siRNA, small interfering RNA; WT, wild type.

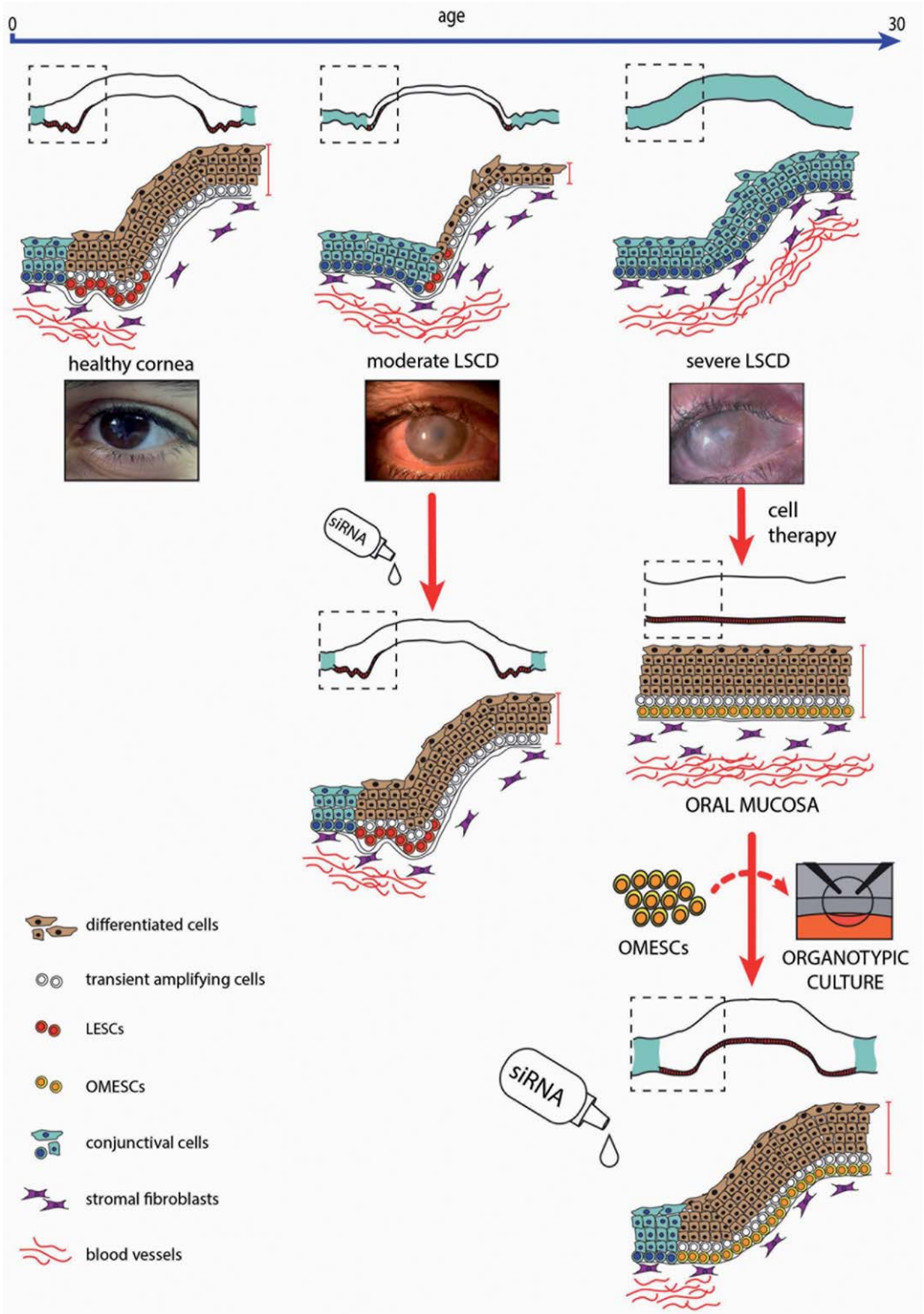

Figure 6. Model of siRNA-based therapeutic approach for LSCD treatment in ectrodactyly-ectodermal dysplasia-clefting (EEC) patients. p63-defective-LESCs have a reduced ability to repopulate the corneal epithelium, which leads to progressive visual impairment culminating in complete bilateral blindness, associated with conjunctivalization. Gene silencing approaches by means of allele-specific siRNAs is potentially a new way to revert the epithelial defects and, eventually, severe visual loss observed in young and adult EEC patients. In young EEC patients, who still have LESCs in the limbus, eye drops containing mutant-specific siRNAs could counterbalance the loss of stem cells. In adult EEC patients, who have a more severe LSCD and no limbus left, gene correction mediated by continuous supplying of specific siRNAs can improve the clinical outcomes of autologous OMESCs graft. Abbreviations: LESCs, limbal epithelial stem cells; LSCD: limbal stem cell deficiency; OMESCs, oral mucosa epithelial stem cells; siRNA, small interfering RNA.

to correct the underlying genetic defect in *p63* using AS gene silencing. Since transplantation of OMESCs has previously shown to be a valid alternative for reconstructing the ocular surface in bilateral LSCD patients, we initially characterized OMESCs isolated from two EEC patients carrying the most severe mutations affecting the cornea: p.R279H and p.R304Q. Compared to controls, both mutants showed (i) premature clonogenic and proliferative stop; (ii) increased replicative senescence; (iii) altered wound healing properties; (iv) reduction of the capacitative calcium entry and (v) defects in stratification and differentiation, thus resulting in severe epithelial hypoplasia and lack of proper tissue polarity. These characteristics explain some of the clinical features of the ocular surface seen in EEC patients: progressive conjunctivalization of the cornea, recurrent corneal erosions, and ulcers that get worse along with the years.

Characterization of OMESCs and AS gene silencing experiments allowed us to make two important findings. First, OMESCs display a higher self-renewal potential than LESCs, thus supporting further their use as an alternative source of cells for the treatment of LSCD. Second, consistent with the finding that mutant R279H p63 mRNA is more stable than WT [32], we found that ΔNp63α accumulates in OMESCs carrying the p.R279H mutation and its expression declines during the differentiation and senescence processes of primary cells in vitro faster than in WT cells. Considering the role of ΔNp63α in LESCs [1–6], this misregulation may have the functional consequence to induce a premature stop to cell proliferation and to allow the alteration of the differentiation pathway. The accumulation of ΔNp63α in p.R279H OMESCs is, at least in part, due to the increased stability of the transcriptionally inactive R279H mutant [32], that negatively interferes with the p63 autoregulatory loop active in stem cells [42]. The specific silencing of the mutated allele may, therefore, have several advantages and reduce both the amount of transcriptionally inactive p63 and the inhibition of the transactivation of the WT p63, mediated by the R279H protein, which is necessary for the activation of the autoregulation loop. All our experiments pointed toward the efficacy and efficiency of siRNA *a*, as the R279H-ΔNp63α-mutant protein was specifically knocked down by approximately 80% while the WT was stably expressed and unaffected. In addition, siRNA *a*-treated p.R279H OMESCs showed longer life-spans, reduced proliferation properties, and effective ability in correcting the epithelial hypoplasia, thus giving rise to a full thickness stratified and differentiated epithelia.

Depending on the timing and severity of LSCD, our results might have clinical applications both for young and adult EEC patients. EEC-related corneal pathology follows a clear clinical course with LSCD usually manifesting in the second to third decade leading to severe corneal failure in the fourth to fifth decade [2]. This provides a therapeutic window to correct the genetic defect using genetic preventive strategies, which could maintain corneal clarity, prevent blindness, and obviate pain and photophobia. In early corneal disease, with LESCs still present in the limbus, the use of eye drops containing mutant-specific siRNAs may be a practical therapeutic option. In patients with established LSCD and no limbal stem cell population, clinical outcomes may be improved by ex vivo gene correction of OMESCs with p63 mutant-specific siRNAs (Fig. 6).

Conclusion

In summary, we truly believe that our strategy could provide a therapeutic window to correct the EEC defect and the use of genetic preventive strategies could counteract the premature differentiation and the clinical downstream effects of limbal stem cell deficiency usually seen in EEC patient. Our findings could also be applicable to other genetic disorders affecting the ocular surface (e.g., aniridia and corneal dystrophies, such as Meesmann).

Acknowledgments

We thank Dr. Micheal Davidson and Dr. Volker Lohman for providing the plasmids pTAG-RFP-T and pWPI-blr, Dr. Gualtiero Alvisi for technical support in the preparation of plasmids and vectors used in this study, Prof. Franco Bassetto for surgical removal of oral mucosal biopsies and the "Ass. p63 Sindrome EEC International Onlus net. work word communication" patient association. The work was partly supported through grants from the Italian Ministry of Health (GR-2009-1555694, CUP n.: H31J11000260001and GR-2010-2316138, CUP n.: H41J12000100001). The funders had no role in study design, data collection and analysis, decision to publish, or preparation of the manuscript.

Author Contributions

E.D.I.: conception and design, data analysis and interpretation, manuscript writing and final approval of manuscript; V.B.: collection and/or assembly of data, data analysis and interpretation, and manuscript writing; A.A.N., C.D.V., A.M., P.R., V.L., P.N., and M.B.: collection and/or assembly of data; S.F.: data analysis and interpretation and manuscript writing; C.E.W.: provision of study material or patients and manuscript writing; D.P.: provision of study material or patients; G.P. and C.P.: data analysis and interpretation and final approval of manuscript.

Disclosure of Potential Conflicts of Interest

The authors indicate no potential conflicts of interest.

References

1 Di Iorio E, Barbaro V, Ruzza A et al. Isoforms of DeltaNp63 and the migration of ocular limbal cells in human corneal regeneration. Proc Natl Acad Sci USA 2005;102:9523-9528.

2 Di Iorio E, Kaye SB, Ponzin D et al. Limbal stem cell deficiency and ocular phenotype in ectrodactyly-ectodermal dysplasia-clefting syndrome caused by p63 mutations. Ophthalmology 2012;119:74-83.

3 Barbaro V, Confalonieri L, Vallini I et al. Development of an allele-specific real-time PCR assay for discrimination and quantification of p63 R279H mutation in EEC syndrome. J Mol Diagn 2012;14:38-45.

4 Shortt AJ, Secker GA, Notara MD et al. Transplantation of ex vivo cultured limbal epithelial stem cells: A review of techniques and clinical results. Surv Ophthalmol 2007;52:483-502.

5 Daya SM, Ilari FA. Living related conjunctival limbal allograft for the treatment of stem cell deficiency. Ophthalmology 2001;108:126-133.

6 Di Iorio E, Ferrari S, Fasolo A et al. Techniques for culture and assessment of limbal stem cell grafts. Ocul Surf 2010;8:146-153.

7 Santos MS, Gomes JA, Hofling-Lima AL et al. Survival analysis of conjunctival limbal grafts and amniotic membrane transplantation in eyes with total limbal stem cell deficiency. Am J Ophthalmol 2005;140:223-230.
8 Nishida K, Yamato M, Hayashida Y et al. Corneal reconstruction with tissue-engineered cell sheets composed of autologous oral mucosal epithelium. N Engl J Med 2004;351:1187-1196.
9 Burillon C, Huot L, Justin V et al. Cultured autologous oral mucosal epithelial cell sheet (CAOMECS) transplantation for the treatment of corneal limbal epithelial stem cell deficiency. Invest Ophthalmol Vis Sci 2012;53:1325-1331.
10 Chen HC, Chen HL, Lai JY al. Persistence of transplanted oral mucosal epithelial cells in human cornea. Invest Ophthalmol Vis Sci 2009;50:4660-4668.
11 Nakamura T, Endo K, Cooper LJ et al. The successful culture and autologous transplantation of rabbit oral mucosal epithelial cells on amniotic membrane. Invest Ophthalmol Vis Sci 2003;44:106-116.
12 Pellegrini G, Traverso CE, Franzi AT et al. Long-term restoration of damaged corneal surfaces with autologous cultivated corneal epithelium. Lancet 1997;349:990-993.
13 Pellegrini G, Golisano O, Paterna P et al. Location and clonal analysis of stem cells and their differentiated progeny in the human ocular surface. J Cell Biol 1999;145:769-782.
14 Magi S, Nasti AA, Gratteri S et al. Gram-negative endotoxin lipopolysaccharide induces cardiac hypertrophy: Detrimental role of Na(+)-Ca(2+) exchanger. Eur J Pharmacol 2015;746:31-40.
15 Barbaro V, Ferrari S, Fasolo A et al. Reconstruction of a human hemicornea through natural scaffolds compatible with the growth of corneal epithelial stem cells and stromal keratocytes. Mol Vis 2009;15: 2084-2093.
16 Shaner NC, Lin MZ, McKeown MR et al. Improving the photostability of bright monomeric orange and red fluorescent proteins. Nat Methods 2008:5:545-551.
17 Backes P, Quinkert D, Reiss S et al. Role of annexin A2 in the production of infectious hepatitis C virus particles. J Virol 2010;84: 5775–5789.
18 Dull T, Zufferey R, Kelly M et al. A third-generation lentivirus vector with a conditional packaging system. J Virol 1998;72: 8463-8471.
19 Elbashir SM, Harborth J, Lendeckel W et al. Duplexes of 21-nucleotide RNAs mediate RNA interference in cultured mammalian cells. Nature 2001;411:494-498.
20 Barbieri CE, Tang LJ, Brown KA et al. Loss of p63 leads to increased cell migration and up-regulation of genes involved in invasion and metastasis. Cancer Res 2006;66: 7589-7597.
21 Tucci P, Agostini M, Grespi F et al. Loss of p63 and its microRNA-205 target results in enhanced cell migration and metastasis in prostate cancer. Proc Natl Acad Sci USA 2012;109:15312-15317.
22 Carroll DK, Carroll JS, Leong CO et al. p63 regulates an adhesion programme and cell survival in epithelial cells. Nat Cell Biol 2006;8:551-561.
23 Borrelli S, Testoni B, Callari M et al. Reciprocal regulation of p63 by C/EBP delta in human keratinocytes. BMC Mol Biol 2007;8:85.
24 Kolly C, Suter MM, Müller EJ. Proliferation, cell cycle exit, and onset of terminal differentiation in cultured keratinocytes: Pre-programmed pathways in control of C-Myc and Notch1 prevail over extracellular calcium signals. J Invest Dermatol 2005;124:1014-1025.
25 Hennings H, Michael D, Cheng C et al. Calcium regulation of growth and differentiation of mouse epidermal cells in culture. Cell 1980;19:245-254.
26 Yuspa SH, Kilkenny AE, Steinert PM et al. Expression of murine epidermal differentiation markers is tightly regulated by restricted extracellular calcium concentrations in vitro. J Cell Biol 1989;109:1207-1217.
27 Rosenthal DS, Steinert PM, Chung S et al. A human epidermal differentiation-specific keratin gene is regulated by calcium not by negative modulators of differentiation in transgenic mouse keratinocytes. Cell Growth Differ 1991;2:107-113.
28 Elsholz F, Harteneck C, Muller W et al. Calcium - A central regulator of keratinocyte differentiation in health and disease. Eur J Dermatol 2014;24:650-661.
29 Bikle DD, Xie Z, Tu CL. Calcium regulation of keratinocyte differentiation. Expert Rev Endocrinol Metab 2012;7:461-472.
30 Dubé J, Rochette-Drouin O, Lévesque P et al. Human keratinocytes respond to direct current stimulation by increasing intracellular calcium: Preferential response of poorly differentiated cells. J Cell Physiol 2012;227: 2660-2667.
31 Parekh AB, Putney JW Jr. Store-operated calcium channels. Physiol Rev 2005;85:757-810.
32 Browne G, Cipollone R, Lena AM et al. Differential altered stability and transcriptional activity of ΔNp63 mutants in distinct ectodermal dysplasias. J Cell Sci 2011;124: 2200-2207.
33 Moretti F, Marinari B, Lo Iacono N et al. A regulatory feedback loop involving p63 and IRF6 links the pathogenesis of 2 genetically different human ectodermal dysplasias. J Clin Invest 2010;120:1570-1577.
34 Barbaro V, Testa A, Di Iorio E et al. C/EBP delta regulates cell cycle and self-renewal of human limbal stem cells. J Cell Biol 2007;177:1037-1049.
35 Elmén J, Thonberg H, Ljungberg K et al. Locked nucleic acid (LNA) mediated improvements in siRNA stability and functionality. Nucleic Acids Res 2005;33:439-447.
36 Mook OR, Baas F, de Wissel MB et al. Evaluation of locked nucleic acid-modified small interfering RNA in vitro and in vivo. Mol Cancer Ther 2007;6:833-843.
37 Gonzalez-Alegre P, Miller VM, Davidson BL et al. Toward therapy for DYT1 dystonia: Allele-specific silencing of mutant TorsinA. Ann Neurol 2003;53:781-787.
38 Rodriguez-Lebron E, Paulson HL. Allele-specific RNA interference for neurological disease. Gene Ther 2006;13:576-581.
39 Atkinson SD, McGilligan VE, Liao H et al. Development of allele-specific therapeutic siRNA or keratin 5 mutations in epidermolysis bullosa simplex. J Invest Dermatol 2011; 131:2079-2086.
40 Leslie Pedrioli DM, Fu DJ, Gonzalez-Gonzalez E et al. Generic and personalized RNAi-based therapeutics or a dominant-negative epidermal fragility disorder. J Invest Dermatol 2012;132:1627-1635.
41 Allen EH, Atkinson SD, Liao H et al. Allele-specific siRNA silencing for the common keratin 12 founder mutation in Meesmann epithelial corneal dystrophy. Invest Ophthalmol Vis Sci 2013;54:494-502.
42 Antonini D, Rossi B, Han R et al. An autoregulatory loop directs the tissue-specific expression of p63 through a long-range evolutionarily conserved enhancer. Mol Cell Biol 2006;26:3308-3318.

See www.StemCells.com for supporting information available online.